Pediatr Radiol (2015) 45:1480–1488
DOI 10.1007/s00247-015-3345-5

ORIGINAL ARTICLE

Ultrasound shear wave speed measurements correlate with liver fibrosis in children

Jonathan R. Dillman[1] · Amer Heider[2] · Jacob L. Bilhartz[3] · Ethan A. Smith[1] · Nahid Keshavarzi[4] · Jonathan M. Rubin[5] · M. James Lopez[3]

Received: 18 November 2014 / Revised: 9 February 2015 / Accepted: 18 March 2015 / Published online: 8 April 2015

Abstract
Background Little published research has shown the relationship between noninvasive US shear wave speed (SWS) measurements and degree of liver fibrosis as established by percutaneous biopsy in children.
Objective To assess the relationship between liver US shear wave speed (SWS) measurements and parenchymal fibrosis in children.
Materials and methods Sixty-two children (0–18 years old) with known or suspected liver disease underwent same-day US shear wave elastography (SWE) and clinically ordered percutaneous core needle biopsy. SWE was performed just before the liver biopsy in the area targeted for sampling, using an Acuson S3000 US system with a 9L4 transducer; six SWS measurements were acquired using Virtual Touch Quantification (VTQ) and Virtual Touch IQ (VTIQ) modes. Biopsy specimens were scored for histological fibrosis and inflammation. Bivariate relationships were assessed using Pearson correlation, while multiple linear regression analysis was used to establish the relationship between SWS and predictor variables. Receiver operating characteristic (ROC) curves were created to assess the abilities of VTQ and VTIQ to discern low vs. high liver fibrosis (histological fibrosis scores 0–2 vs. 3–6).
Results There were significant positive correlations between liver histological fibrosis score and VTQ (n=49) and VTIQ (n=48) mean shear wave speed measurements (r=0.68 and r=0.73; P-values <0.0001). There also were significant positive correlations between liver histological inflammation score and VTQ and VTIQ mean shear wave speed measurements (r=0.47 and r=0.44, and P=0.0006 and P=0.0016, respectively). For VTQ, both histological fibrosis (P<0.0001) and inflammation (P=0.04) scores were significant predictors of shear wave speed (model adjusted R^2=0.49). For VTIQ, only histological fibrosis score (P<0.0001) was a significant predictor of shear wave speed (model adjusted R^2=0.56). ROC areas under the curve were 0.84 and 0.86 for VTQ and VTIQ, respectively.
Conclusion Liver US shear wave speed measurements increase with increasing parenchymal fibrosis in children.

Keywords Acoustic radiation force impulse (ARFI) · Children · Comparative study · Fibrosis · Inflammation · Liver · Shear wave elastography · Ultrasonography

This article was awarded the John Caffey Award for Best Clinical Research Paper at the Society for Pediatric Radiology 2014 meeting.

✉ Jonathan R. Dillman
jonadill@med.umich.edu

[1] Department of Radiology, University of Michigan Health System, Section of Pediatric Radiology, C. S. Mott Children's Hospital, 1540 E. Hospital Drive, Ann Arbor, MI 48109, USA

[2] Department of Pathology, University of Michigan Health System, Ann Arbor, MI, USA

[3] Division of Pediatric Gastroenterology, Department of Pediatrics, University of Michigan Health System, Ann Arbor, MI, USA

[4] Michigan Institute for Clinical and Health Research, University of Michigan, Ann Arbor, MI, USA

[5] Division of Abdominal Radiology, Department of Radiology, University of Michigan Health System, Ann Arbor, MI, USA

Introduction

There are many causes of chronic liver disease in children [1–3]. Over time, repetitive hepatocyte injury can lead to the deposition of parenchymal fibrosis, or scarring. Pediatric liver fibrosis is frequently progressive, with the extent of fibrosis increasing (often unpredictably) over time, sometimes culminating in cirrhosis. Common offending conditions include biliary atresia (both untreated and following Kasai portoenterostomy), total-parenteral-nutrition-related liver disease, cystic fibrosis, non-alcoholic fatty liver disease (NAFLD), sclerosing cholangitis, autoimmune hepatitis, a variety of metabolic disorders, and cryptogenic cirrhosis [1–3].

Several imaging modalities, including US, MRI and CT, can identify end-stage liver fibrosis, or overt cirrhosis. Cirrhosis may be suggested by anatomical imaging based on changes in the liver morphology (e.g., the liver commonly appears shrunken and has a nodular surface) or changes in signal intensity using conventional MRI techniques [4]. MR elastography has recently been explored in children and adults with chronic liver disease, including pediatric patients with NAFLD and post-Fontan palliation for congenital heart disease, and has documented increased liver stiffness in the presence of fibrosis [5–7]. MR elastography has limitations, however, including high cost (per examination and related to necessary infrastructure), limited availability, need for sedation or general anesthesia in some patients, and MR signal loss in the setting of iron overload [5].

No routinely employed imaging modality can detect and accurately quantify mild to moderate amounts of liver fibrosis or assess for progression of fibrosis over time. Consequently, liver biopsy, often using a laparoscopic or US-directed percutaneous core needle approach [8–10], is commonly required to confirm the presence and measure the amount of fibrosis in children. This procedure has limitations, such as poor patient and parent acceptance, extremely limited sampling of the liver, need for sedation or general anesthesia, and a variety of procedural risks, including life-threatening hemoperitoneum [5, 10].

Recently, quantitative US-based shear wave elastography (SWE) techniques have become available in the United States that allow for noninvasive assessment of liver stiffness. These techniques have numerous advantages in children because they allow rapid assessment, do not require ionizing radiation, are increasingly integrated into state-of-the-art US systems, cost less than MR elastography, and do not require sedation or general anesthesia. Furthermore, US shear wave elastography is a portable technique that can allow imaging in the radiology department or clinic and at the bedside. To date, a relatively small number of studies have evaluated the use of US shear wave elastography for detecting liver fibrosis in children [11–15]. Acoustic radiation force impulse (ARFI) SWE techniques use US force to generate transient tissue deformations that give rise to in vivo shear waves in an organ of interest (e.g., liver). Shear wave speed (SWS) then can be measured (in m/s) using the same US transducer to provide an estimate of tissue stiffness (hardness). SWS increases with increasing tissue stiffness and can be directly related to Young's modulus (kPa). KPa, a material property that describes a material's elastic stiffness, is presented by some vendors and is approximately $3 \times (\text{shear wave speed in m/s})^2$ [16].

The purpose of our study was to prospectively assess the relationship between US-derived liver shear wave speed and parenchymal fibrosis (based on temporally related, anatomically related histology) in children for two different SWE techniques. In addition, we sought to model the relationship between liver SWS and a variety of predictor variables, including histological fibrosis, histological inflammation, age and gender.

Materials and methods

This investigation was approved by the institutional review board and complies with the Health Insurance Portability and Accountability Act.

Sixty-two children (0–18 years of age) undergoing US-directed clinically ordered percutaneous core needle liver biopsy for known or suspected (non-neoplastic) liver disease were included in this prospective study. Children were enrolled between November 2012 and July 2014. We obtained parental/guardian informed consent for all study participants; we obtained subject assent for children older than 10 years. Some data from 11 children in this investigation were previously presented in a recent study that used shear wave elastography to help differentiate biliary atresia from other causes of neonatal/infantile jaundice [12].

Following the initiation of conscious sedation or induction of general anesthesia, US shear wave elastography was performed in either the interventional radiology suite or operating room just before US-directed percutaneous core needle liver biopsy. SWE was performed in the area of the liver targeted for biopsy. All study US examinations were performed by a small group of dedicated pediatric US technologists trained in shear wave elastography under the supervision of a research assistant. All examinations were conducted using an Acuson S3000 system and 9L4 transducer (Siemens Medical Solutions USA, Malvern, PA). SWE was performed with the child supine and free-breathing unless the child was old enough and able to follow a command to breath-hold. We used two methods: Virtual Touch Quantification (VTQ) and Virtual Touch IQ (VTIQ) (Fig. 1). VTQ and VTIQ are vendor-specific terms for two methods of shear wave elastography, also known as acoustic radiation force imaging (ARFI). The exact imaging approach (e.g., right versus left lobe, intercostal versus subcostal) for a given child was determined by the

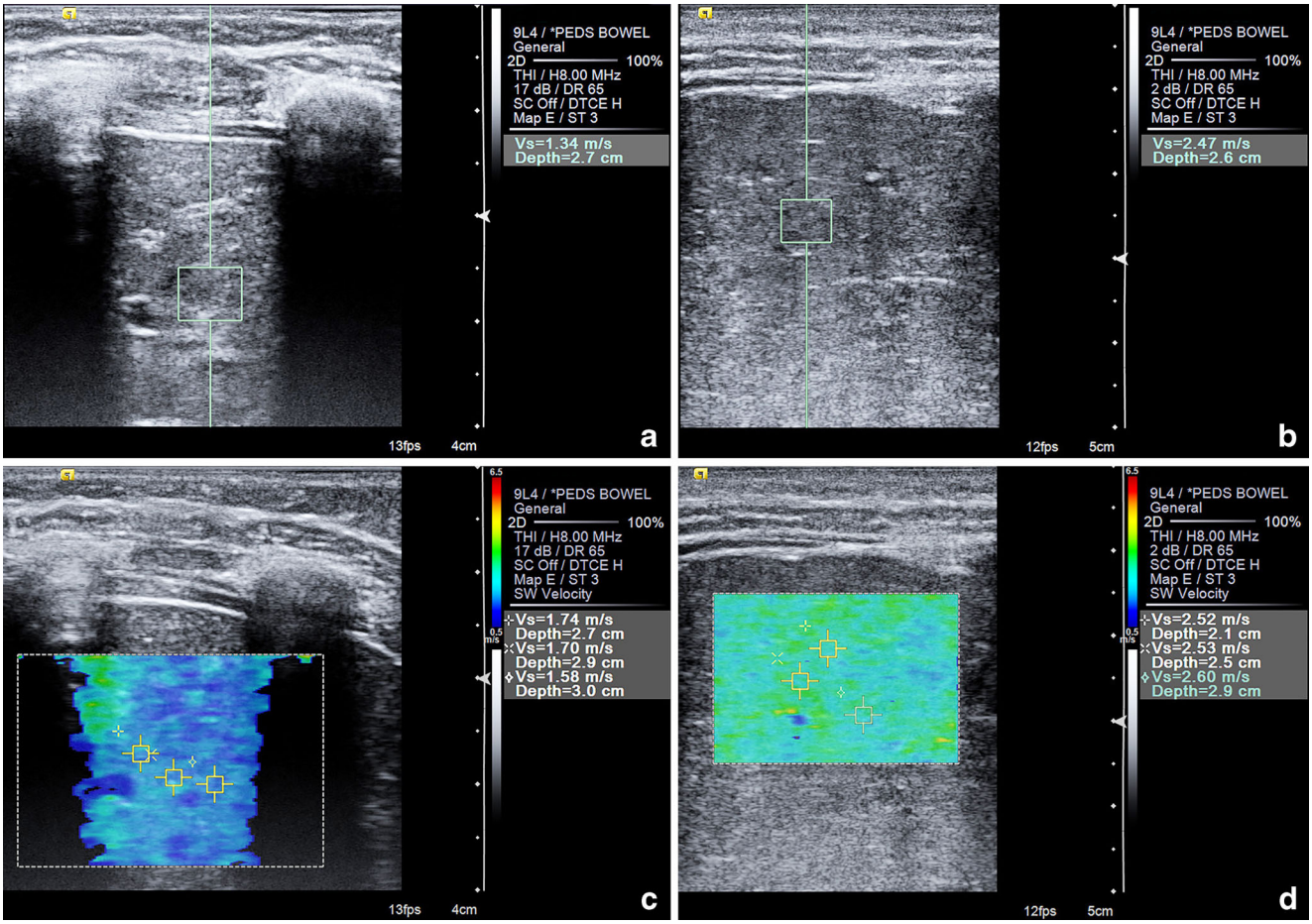

Fig. 1 Shear wave elastography. Virtual Touch Quantification (VTQ) mode images in (**a**) a 5-year-old boy and (**b**) a 17-year-old girl. Virtual Touch IQ (VTIQ) shear wave elastography mode images in (**c**) the same girl and (**d**) the same boy as (**a** and **b**). Higher shear wave speed measurements (and elastogram heterogeneity on VTIQ imaging) correlate with increasing parenchymal fibrosis

gastroenterologist or interventional radiologist supervising the liver biopsy procedure. Because all biopsy procedures were performed under conscious sedation or general anesthesia, subjects were nil per os during SWE in accordance with Department of Anesthesia guidelines.

The VTQ shear wave elastography mode uses an operator-placed 4.0-MHz ARFI or "push pulse" to remotely produce shear waves within an organ of interest, while the VTIQ mode uses multiple ARFIs (4.0–5.7 MHz, arising from different locations along the transducer face and focused at multiple depths) to produce shear waves and create a color image (elastogram) of tissue stiffness. VTQ using the 9L4 transducer allows placement of a single fixed-size 5-mm^2 region of interest (ROI) per acquired image in order to measure shear wave speed (m/s), while VTIQ allows placement of multiple fixed-size 1.5-mm^2 ROIs per acquired image in order to measure shear wave speed. Shear wave elastography was performed using the US system's default settings; VTIQ color elastogram scale ranged from 0.5 m/s (blue) to 6.5 m/s (red).

When using the VTQ mode, regions of interest were placed in the liver in the area targeted for biopsy, avoiding visible blood vessels and at least 10 mm below the liver surface. Six VTQ shear wave speed measurements were acquired from each child, with the transducer removed and replaced for each image acquisition. When using the VTIQ mode, two elastogram images of the liver were obtained in the area targeted for biopsy. Six VTIQ shear wave speed measurements also were acquired from each subject (three measurements per elastogram, with regions of interest placed at the discretion of the US technologist in areas of "complete color fill-in"). All SWE images were obtained with the smallest amount of transducer pressure needed to allow diagnostic imaging.

Age, gender and body mass index (BMI) were documented for each child. We reviewed electronic medical records to obtain the clinical indications for liver biopsy as well as histological diagnoses.

Histological liver analysis

All children in our study underwent clinically ordered US-directed core needle liver biopsy procedures using either a

16- or 18-gauge biopsy device (Bard Monopty disposable core biopsy instrument; Bard Biopsy Systems, Tempe, AZ). At least two core tissue specimens were acquired from each child. After routine tissue processing, specimens were placed on glass slides and stained with hematoxylin and eosin as well as Masson trichrome. Tissue specimens were scored for histological fibrosis (Ishak fibrosis staging system, 0–6, where 0 indicates no fibrosis and 6 indicates cirrhosis) and inflammation (modified hepatitis activity index, 0–18, where 0 indicates no inflammation and 18 indicates severe inflammation and necrosis); scoring was conducted by a board-certified pediatric pathologist (with 3 ½years of experience) blinded to US shear wave elastography results [17, 18]. These histological scoring systems were employed because they have been used and validated in numerous adult studies; there are no similar commonly used pediatric instruments for scoring histological inflammation and fibrosis.

Statistical analysis

Continuous data were summarized using means and standard deviations, while categorical data were summarized using counts and percentages. Bivariate relationships, including VTQ and VTIQ shear wave speed (individual subject mean, median and maximum) vs. histological fibrosis and inflammation scores were assessed using Pearson correlation. Analysis of variance (ANOVA) was used to compare VTQ and VTIQ mean shear wave speed measurements in children with no/mild vs. moderate vs. extensive fibrosis (histological fibrosis scores 0–1 vs. 2–3 vs. 4–6). These means also were compared in a pairwise manner using the Tukey multiple comparison test with appropriate *P*-value adjustment.

We used multiple linear regression analysis to assess the relationship between SWS and predictor variables (histological fibrosis and inflammation scores as well as age and gender) for both VTQ and VTIQ. The Akaike Information Criterion was used for final model selection. Receiver operating characteristic (ROC) curves were created to assess the diagnostic performances of VTQ and VTIQ for discriminating low (histological fibrosis scores 0–2) vs. high (histological fibrosis scores 3–6) fibrosis. All inference testing was performed using SAS version 9.3 (SAS Institute, Cary, NC). A *P*-value <0.05 was considered significant.

Results

Subject characteristics

Sixty-two children were included in our study, 29 (47%) girls and 33 (53%) boys. Mean subject age was 8.0±5.8 years (range, 4 weeks–18 years). Clinical indications for liver biopsy as well as histological diagnoses are presented in Table 1.

Table 1 Clinical indications for liver biopsy and final diagnoses in 62 children

Indication for biopsy	*n*	Final diagnosis	*n*
Prior orthotopic liver transplantation (OLT)	24	OLT rejection	11
Elevated liver function tests (native liver)	21	Nonspecific liver abnormality	10
Cholestasis	11	Normal liver	9
Elevated liver function tests (post Kasai procedure)	1	Biliary atresia/biliary obstruction	8
Known autoimmune hepatitis	1	Autoimmune hepatitis	5
Known cryptogenic cirrhosis	1	Sclerosing cholangitis	5
Known glycogen storage disease	1	Drug-induced hepatitis	2
Known pyruvate kinase deficiency	1	Glycogen storage disease	2
Known sclerosing cholangitis	1	Neonatal hepatitis	2
		Non-alcoholic steatohepatitis	2
		Paucity of bile ducts	2
		Cryptogenic cirrhosis	1
		Congenital hepatic fibrosis	1
		Leukemia	1
		Viral hepatitis	1

VTQ was successful (meaning shear wave speed measurements could be acquired) in 49 children, including 24 (49%) girls and 25 (51%) boys, using a 9L4 transducer. Mean subject age was 7.2±5.5 years. Children (5 girls and 8 boys) with non-diagnostic VTQ imaging had a mean age of 11.1 years. Mean body mass index (BMI) for children with successful VTQ imaging was 18.4±4.7 kg/m^2 vs. 30.4±6.4 kg/m^2 for children with unsuccessful imaging (P<0.0001).

VTIQ was successful (meaning that more than two-thirds of the elastogram box filled with color data based on subjective assessment) in 48 children, including 21 (44%) girls and 27 (56%) boys. Mean subject age was 6.7±5.5 years. Children (8 girls and 6 boys) with non-diagnostic VTIQ imaging had a mean age of 12.4 years. Mean BMI for children with successful VTIQ imaging was 17.6±4.1 kg/m^2 vs. 27.8±7.1 kg/m^2 for children with unsuccessful imaging (P=0.0001).

Bivariate relationships

There were significant positive correlations between individual subject mean, median and maximum VTQ shear wave speed measurements and both histological fibrosis and inflammation scores (Table 2) (Fig. 2). Similarly, there were significant positive correlations between individual subject mean, median and maximum VTIQ shear wave speed measurements and both histological

Table 2 Pearson correlation (r) between individual subject shear wave speed measurements (in m/s, n=6) and predictor variables, including histological fibrosis score (0–6), histological inflammation score (0–18) and age

r (P-value) (n)	VTQ – mean SWS	VTQ – median SWS	VTQ – max SWS	VTIQ – mean SWS	VTIQ – median SWS	VTIQ – max SWS
Fibrosis score	0.68	0.63	0.65	0.73	0.72	0.68
	(<0.0001)	(<0.0001)	(<0.0001)	(<0.0001)	(<0.0001)	(<0.0001)
	(49)	(49)	(49)	(48)	(48)	(48)
Inflammation score	0.47	0.45	0.52	0.44	0.44	0.48
	(0.0006)	(0.001)	(0.0001)	(0.0016)	(0.002)	(0.0006)
	(49)	(49)	(49)	(48)	(48)	(48)
Age	0.02	−0.02	0.07	−0.28	−0.27	−0.26
	(0.87)	(0.86)	(0.63)	(0.057)	(0.06)	(0.08)
	(49)	(49)	(49)	(48)	(48)	(48)

max maximum, *SWS* shear wave speed, *VTIQ* Virtual Touch IQ, *VTQ* Virtual Touch Quantification

fibrosis and inflammation scores (Table 2) (Fig. 2). VTQ and VTIQ mean shear wave speed measurements were also highly positively correlated, as expected (r= 0.79; P<0.0001) (Fig. 3). There was no significant correlation between SWS measurements (mean, median and maximum) and age using VTQ. There were marginally significant negative correlations between SWS measurements (mean, median and maximum) and age using VTIQ (P-values 0.057–0.08).

Analysis of variance (ANOVA)

There was a significant difference in the mean SWS among children with Ishak 0–1 (n=28, 1.46±0.23 m/s), 2–3 (n=11, 1.82±0.50 m/s) and 4–6 (n=10, 2.15±0.21 m/s) histological fibrosis scores using VTQ (P<0.0001) (Fig. 4). Similarly, there was a significant difference in the mean SWS among children with Ishak 0–1 (n=29, 1.74±0.18 m/s), 2–3 (n=10, 2.02±0.44 m/s) and 4–6 (n=9, 2.87±0.75 m/s) histological fibrosis scores using VTIQ (P<0.0001) (Fig. 4). Pairwise comparison testing of mean shear wave speeds among histological fibrosis score groups with Tukey-adjusted P-values is presented in Table 3.

Predicting liver shear wave speed

We used multiple linear regression to assess the relationship between liver SWS (mean) and predictor variables (histological liver fibrosis and inflammation scores as well as age and gender) for both VTQ and VTIQ.

VTQ

For VTQ, histological fibrosis and inflammation scores were significant predictors of mean shear wave speed (P<0.0001 and P=0.04, respectively). Age and gender were not significant predictors, and they caused the Akaike

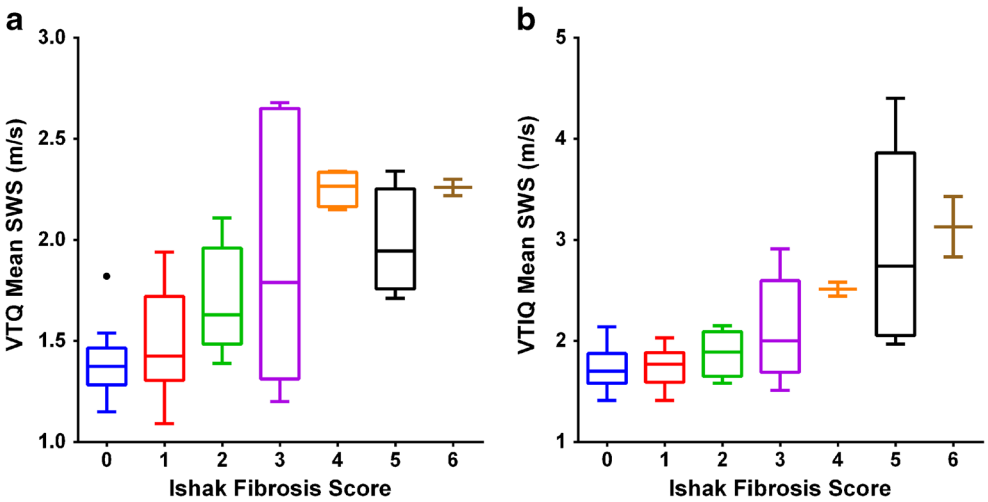

Fig. 2 Comparison of shear wave speed (SWS) and fibrosis. Box plots show increasing liver mean SWS measurements with increasing parenchymal fibrosis using (**a**) VTQ and (**b**) VTIQ shear wave elastography modes. *VTIQ* Virtual Touch IQ, *VTQ* Virtual Touch Quantification

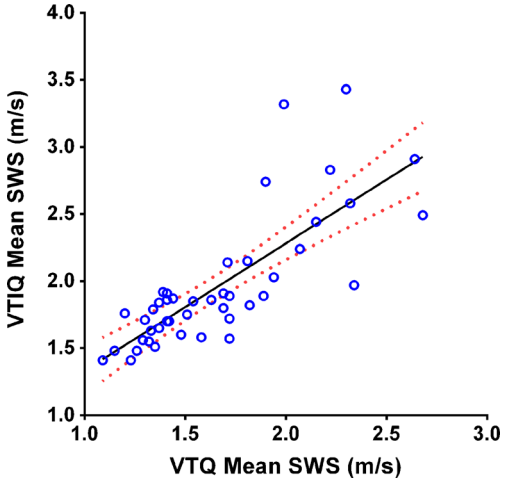

Fig. 3 Correlations between Virtual Touch Quantification (VTQ) and Virtual Touch IQ (VTIQ) shear wave speed measurements. Scatter plot (with fit line and 95% confidence interval) shows the relationship between VTQ and VTIQ mean shear wave speed (SWS) measurements in 44 children (r=0.79; P<0.0001)

Information Criterion to undesirably increase. The final model was as follows: SWS (m/s)=1.32+(0.13×histological fibrosis score)+(0.025 × histological inflammation score) (P<0.0001; adjusted-R^2=0.49).

VTIQ

For VTIQ, histological fibrosis score was the only significant predictor of mean shear wave speed (P<0.0001). Histological inflammation score (P=0.09) and age (P=0.10) were marginally significant predictors and were included in the final model, because they caused the Akaike Information Criterion to decrease. Gender was not a significant predictor and caused the Akaike Information Criterion to undesirably increase. The final model was as follows: SWS (m/s)=1.65+(0.20 × histological fibrosis score)+(0.028 × histological inflammation score)+(−0.018 × age) (P<0.0001; adjusted-R^2=0.56).

Table 3 Pairwise comparison of mean shear wave speed measurements in the liver among children with low, moderate and extensive histological fibrosis

Histological fibrosis groups being compared	Mean SWS difference (m/s)	Significant?	Adjusted P-value*
VTQ			
0–1 vs. 2–3	0.36	Yes	0.006
0–1 vs. 4–6	0.69	Yes	<0.0001
2–3 vs. 4–6	0.33	Yes	0.045
VTIQ			
0–1 vs. 2–3	0.27	No	0.15
0–1 vs. 4–6	1.13	Yes	<0.0001
2–3 vs. 4–6	0.86	Yes	<0.0001

SWS shear wave speed, *VTIQ* Virtual Touch IQ, *VTQ* Virtual Touch Quantification

*P-values are adjusted using the Tukey method

Receiver operating characteristic (ROC) curve analysis

Receiver operating characteristic (ROC) analysis was performed to assess the ability of shear wave speed to discriminate children with low vs. high liver fibrosis histological scores. For VTQ, the area under the curve was 0.84 (95% CI: 0.70–0.98; P=0.0001) (Fig. 5). A shear wave speed cut-off value of 2.07 m/s gave rise to an excellent positive likelihood value (20.6) for detecting a high histological fibrosis score, with a sensitivity of 63% and specificity of 97%. For VTIQ, the area under the curve was 0.86 (95% CI: 0.72–1.0; P<0.0001) (Fig. 5). An SWS cut-off value of 2.15 m/s gave rise to an excellent positive likelihood value (22.0) for

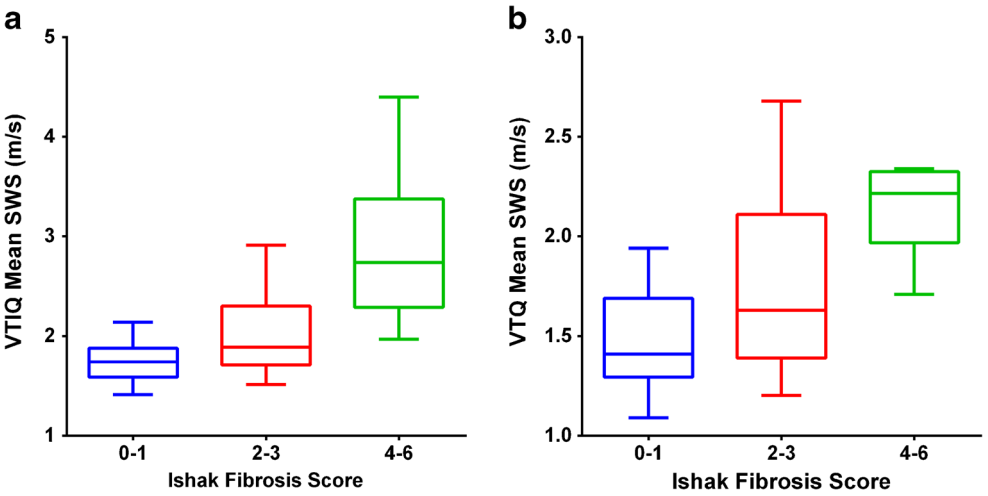

Fig. 4 Shear wave speed measurements compared to histological fibrosis scores. Box plots show mean shear wave speed (SWS) measurements for children with differing amounts of liver fibrosis using (**a**) VTIQ and (**b**) VTQ modes. Both imaging modes demonstrate increases in SWS with increasing histological fibrosis score (P<0.0001 for both VTQ and VTIQ). *VTIQ* Virtual Touch IQ, *VTQ* Virtual Touch Quantification

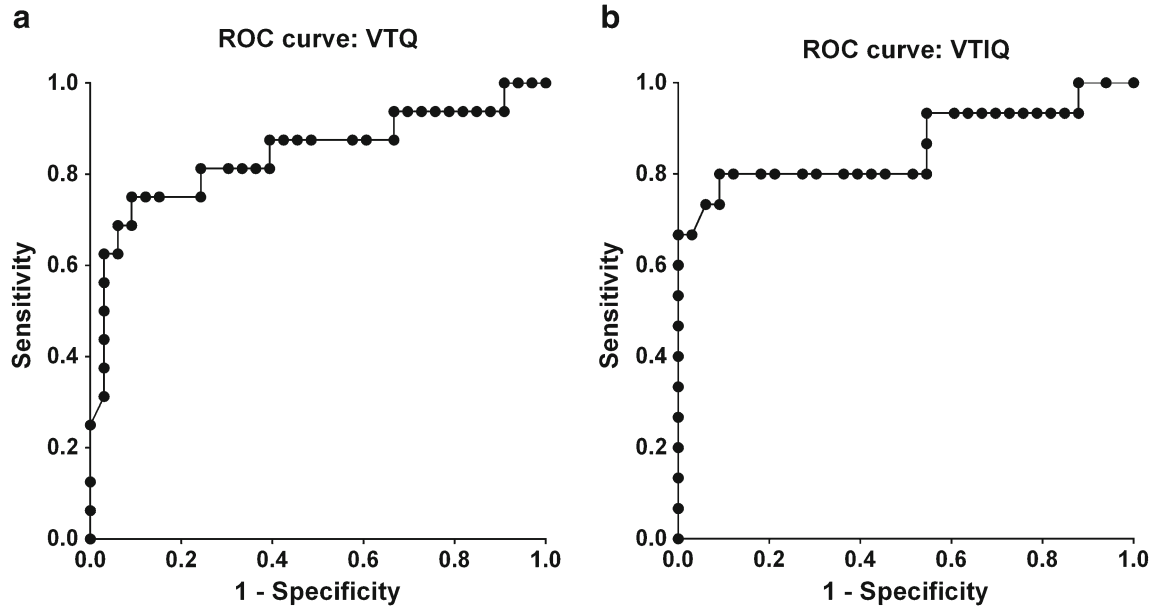

Fig. 5 Receiver operating characteristic (ROC) curves for discriminating low (histological fibrosis scores 0–2) vs. high (histological fibrosis scores 3–6) liver fibrosis using mean shear wave speed. **a** Area under the curve for VTQ is 0.84 (95% CI: 0.70–0.98). **b** Area under the curve for VTIQ is 0.86 (95% CI: 0.72–1.0). *VTIQ* Virtual Touch IQ, *VTQ* Virtual Touch Quantification

detecting high histological fibrosis score, with a sensitivity of 67% and specificity of 97%.

Discussion

Diagnostic SWS measurements could be obtained in 49 of 62 (79%) children using VTQ and 48 of 62 (77%) children using VTIQ. A review of unsuccessful cases (that is children in whom shear wave speed measurements could not be obtained for VTQ — the display presents an error message in these instances — or in whom less than two-thirds of the elastogram box filled with color data for VTIQ) showed that these children were generally older and larger in body habitus compared to children with diagnostic SWE imaging. Interestingly, some children with unsuccessful VTQ imaging had successful VTIQ imaging, and vice versa, a phenomenon that is of uncertain explanation. Increased abdominal wall adipose tissue can attenuate sound waves with resultant smaller applied radiation forces, poor signal and failure to generate a diagnostic shear wave speed estimate [19]. A small percentage of non-diagnostic cases probably were result of severe respiratory motion, which likely hindered shear wave tracking. In the setting of unsuccessful US SWE of the liver, MR elastography is a viable alternative, particularly in larger pediatric patients, such as children with NAFLD [7]. We intentionally chose to image children with only a 9L4 linear transducer to minimize measurement error, because imaging with more than one transducer adds a potential source of variability when trying to correlate SWS measurements with histological findings given that shear wave speed measurements are slightly transducer-dependent [20]. However, it should be noted that VTQ SWE can also be performed with a 4C1 convex transducer, which has a lower-frequency push pulse and is optimized to image the liver in larger children and adults. At this time, only the 9L4 linear transducer is compatible with SWE in VTIQ mode.

Bivariate analyses showed significant positive correlations between SWS measurements and both histological fibrosis and inflammation for VTQ and VTIQ. Although the relationship between SWS and histological fibrosis score was quite strong for both SWE modes, the relationship between SWS and histological inflammation score was not inconsequential. Our multivariate regression models suggest that histological inflammation affects liver SWS when adjusted for amount of liver fibrosis. Interestingly, very similar strengths of correlation were observed between individual subject mean, median and maximum SWS measurements and histological fibrosis and inflammation scores for both VTQ and VTIQ.

ANOVA testing also showed that liver SWS increases with increasing liver fibrosis. However, box plots constructed using three levels of liver fibrosis (histological fibrosis scores 0–1 vs. 2–3 vs. 4–6) showed some overlap of SWS measurements for each histological category. Thus it is unlikely that SWE (or at least VTQ and VTIQ in their current forms) can differentiate between certain amounts of histological fibrosis with a high degree of accuracy (e.g., Ishak fibrosis score 1 vs. 2, 2 vs. 3, or 3 vs. 4). ROC curve analyses show that certain SWS

thresholds can offer reasonable sensitivity and very high specificity for discriminating no/mild (low) fibrosis from moderate/severe (high) fibrosis. ROC areas under the curve were similar for VTQ and VTIQ (0.84 and 0.86, respectively). It should be noted that threshold SWS values for discriminating histological levels of fibrosis may be vendor-specific to some extent based on recent phantom data experiments by the Quantitative Imaging Biomarker Alliance [21]. This collaborative research group showed that "there is a statistically significant difference in SWS estimates among [various ultrasound] systems." Ultimately SWE is likely to be most useful for determining the presence vs. absence of substantial liver fibrosis and for monitoring fibrosis progression over time (as opposed to determining the exact amount of fibrosis present).

Multiple linear regression analysis was used to assess relationships between liver SWS and a variety of predictor variables, including histological fibrosis score, histological inflammation score, age and gender. For VTQ, *both* histological fibrosis and inflammation scores were significant predictor variables; the contribution of histological inflammation score is an important observation and suggests that factors other than fibrosis can impact liver shear wave speed measurements. When adjusted for histological inflammation score, an increase in histological fibrosis score by 1 unit (e.g., going from Ishak fibrosis score of 3 to 4) causes a 0.13-m/s increase in mean SWS, on average. For VTIQ, histological fibrosis score was the only significant predictor variable, although histological inflammation score and age improved overall model quality. When adjusted for histological inflammation score and age, an increase in histological fibrosis score by 1 unit causes a 0.20-m/s increase in mean SWS, on average.

For VTIQ, the final multiple linear regression model had an adjusted-R^2 value of 0.56. This means that approximately 56% of the variation in mean SWS observed in the children in our study can be explained by our model and its predictor variables; however, 44% of the variation remains unexplained. This unexplained variability is likely a result of several factors, including measurement variability related to the SWE technique used (variability inherent to VTIQ, for example), variability in tissue sampling and histological scoring, and individual subject biological variability. In addition, we assumed a linear relationship between SWS and histological fibrosis and inflammation scores. It may be that these relationships are more complex than we appreciate, with SWS increasing nonlinearly with increasing parenchymal fibrosis or inflammation.

A major strength of our investigation is that it may be the first to directly compare the VTQ and VTIQ SWE modes in the assessment of pediatric liver fibrosis. VTIQ, unlike VTQ, provides a color image of liver stiffness, allowing identification of the stiffest areas of the liver and assessment of parenchymal heterogeneity. Our results suggest that, on average in children, VTIQ SWS measurements are slightly higher than VTQ measurements in the same individual. The source of this systematic difference is not exactly certain, although it likely has to do with technical differences between the VTQ and VTIQ modes. Going forward, as SWE is clinically implemented in both children and adults, it will be important to account for differences in SWS measurements obtained using different SWE modes and different US systems in order to properly interpret results. Because our study has nearly 30 children with no or very minimal liver fibrosis (histological fibrosis scores 0–1), our results should help establish expected normative/near-normative SWS values for the specific US system we used in the pediatric population (approximately 1.46 m/s [95% CI: 1.37–1.55 m/s] for VTQ and 1.74 m/s [95% CI: 1.67–1.81 m/s] for VTIQ). These SWS values are slightly higher than those reported in some published studies. For example, a recent study by Matos et al. [22] using VTQ and a 4C1 transducer determined normal pediatric liver SWS to be 1.07 m/s, on average, while a study by Fontanilla et al. [23] using a 9L4 transducer found normal pediatric liver SWS to be 1.15 m/s, on average. Another recent study, by Tutar et al. [15], using a different US system (SuperSonic Imagine, Aix-en-Provence, France) determined normal pediatric liver SWS to be 1.56 m/s, quite similar to our results.

Our study has a few limitations. First, about half of the children in our study had no or very minimal liver fibrosis, while smaller percentages of had higher degrees of fibrosis (e.g., only eight children had an Ishak fibrosis score of 5 or 6). Despite this, we have clearly demonstrated that liver SWS measurements increase with increasing inflammation and fibrosis. A larger number of children with moderate-severe liver fibrosis would have allowed us to even more accurately model the relationship between SWS and histological fibrosis score. Second, our results could be impacted by the fact our investigation used a single pathologist to score histological inflammation and fibrosis. Histological staging of fibrosis and inflammation is subjective, despite the use of validated semi-quantitative scoring systems, and is potentially susceptible to systematic and random measurement errors. Finally, although we performed SWE in the area of tissue sampling at the time of biopsy, it is still nearly impossible to attain perfect 1:1 imaging-to-histology correlation.

Conclusion

Liver SWS measurements increase with increasing hepatic fibrosis in children. VTQ and VTIQ shear wave speed measurements are highly correlated, and liver SWS measurements can reasonably discriminate children with no or mild liver fibrosis from those with moderate or severe liver fibrosis. Using multiple linear regression analysis, we have also shown that *both* histological fibrosis and inflammation cause

predictable increases in US-derived SWS measurements. Additional research is needed to improve the diagnostic accuracy of US SWE as well as to understand how SWS measurements change over time in children with chronic liver disease, how edema and congestion impact liver SWS measurements, and how US SWE results compare to those obtained using MR elastography.

Acknowledgments This study was supported by grant number 2UL1TR000433 from the National Center for Advancing Translational Sciences. The content is solely the responsibility of the authors and does not necessarily represent the official views of NCATS or the National Institutes of Health. Investigator-initiated grant support was also provided by Siemens Medical Solutions USA. This work was presented at the 57th annual meeting of the Society for Pediatric Radiology, Washington, DC, May 2014.

Conflicts of interest None

References

1. Dehghani SM, Imanieh MH, Haghighat M et al (2013) Etiology and complications of liver cirrhosis in children: report of a single center from southern Iran. Middle East J Dig Dis 5:41–46
2. Goss JA, Shackleton CR, McDiarmid SV et al (1998) Long-term results of pediatric liver transplantation: an analysis of 569 transplants. Ann Surg 228:411–420
3. Keller PD, Nute WL Jr (1949) Cirrhosis of the liver in children: a clinical and pathologic study of 40 cases. J Pediatr 34:588–615
4. Dodd GD 3rd, Baron RL, Oliver JH 3rd et al (1999) Spectrum of imaging findings of the liver in end-stage cirrhosis: part I, gross morphology and diffuse abnormalities. AJR Am J Roentgenol 173:1031–1036
5. Taouli B, Ehman RL, Reeder SB (2009) Advanced MRI methods for assessment of chronic liver disease. AJR Am J Roentgenol 193:14–27
6. Wallihan DB, Podberesky DJ, Marino BS et al (2014) Relationship of MR elastography determined liver stiffness with cardiac function after Fontan palliation. J Magn Reson Imaging 40:1328–1335
7. Xanthakos SA, Podberesky DJ, Serai SD et al (2014) Use of magnetic resonance elastography to assess hepatic fibrosis in children with chronic liver disease. J Pediatr 164:186–188
8. Bravo AA, Sheth SG, Chopra S (2001) Liver biopsy. N Engl J Med 344:495–500
9. Esposito C, Garipoli V, Vecchione R et al (1997) Laparoscopy-guided biopsy in diagnosis of liver disorders in children. Liver 17: 288–292
10. Govender P, Jonas MM, Alomari AI et al (2013) Sonography-guided percutaneous liver biopsies in children. AJR Am J Roentgenol 201:645–650
11. Hanquinet S, Rougemont AL, Courvoisier D et al (2013) Acoustic radiation force impulse (ARFI) elastography for the noninvasive diagnosis of liver fibrosis in children. Pediatr Radiol 43:545–551
12. Leschied JR, Dillman JR, Bilhartz J et al (2014) Shear wave elastography helps differentiate biliary atresia from other neonatal/infantile liver diseases. Pediatr Radiol. doi:10.1007/s00247-014-3149-z
13. Monti L, Manco M, Lo Zupone C et al (2012) Acoustic radiation force impulse (ARFI) imaging with virtual touch tissue quantification in liver disease associated with cystic fibrosis in children. Radiol Med 117:1408–1418
14. Shima H, Igarashi G, Wakisaka M et al (2012) Noninvasive acoustic radiation force impulse (ARFI) elastography for assessing the severity of fibrosis in the post-operative patients with biliary atresia. Pediatr Surg Int 28:869–872
15. Tutar O, Beser OF, Adaletli I et al (2014) Shear wave elastography in the evaluation of liver fibrosis in children. J Pediatr Gastroenterol Nutr 58:750–755
16. Palmeri ML, Nightingale KR (2011) Acoustic radiation force-based elasticity imaging methods. Interface Focus 1:553–564
17. Ishak K, Baptista A, Bianchi L et al (1995) Histological grading and staging of chronic hepatitis. J Hepatol 22:696–699
18. Knodell RG, Ishak KG, Black WC et al (1981) Formulation and application of a numerical scoring system for assessing histological activity in asymptomatic chronic active hepatitis. Hepatology 1: 431–435
19. Palmeri ML, Wang MH, Rouze NC et al (2011) Noninvasive evaluation of hepatic fibrosis using acoustic radiation force-based shear stiffness in patients with nonalcoholic fatty liver disease. J Hepatol 55:666–672
20. Dillman JR, Chen S, Davenport MS et al (2014) Superficial ultrasound shear wave speed measurements in soft and hard elasticity phantoms: repeatability and reproducibility using two ultrasound systems. Pediatr Radiol 45:376–385
21. Hall TJ, Milkowski A, Garra B et al (2013) RSNA/QIBA: Shear wave speed as a biomarker for liver fibrosis staging. Radiological Society of North America. http://qibawiki.rsna.org/images/f/fe/IEEE2013_QIBA_2013aug9.pdf. Accessed 9 Feb 2015
22. Matos H, Trindade A, Noruegas MJ (2014) Acoustic radiation force impulse imaging in pediatric patients: normal liver values. J Pediatr Gastroenterol Nutr 59:684–688
23. Fontanilla T, Canas T, Macia A et al (2014) Normal values of liver shear wave velocity in healthy children assessed by acoustic radiation force impulse imaging using a convex probe and a linear probe. Ultrasound Med Biol 40:470–477